

## **An Accessible NDVI Classification Tool for Urban and Suburban Vegetation Change Analysis**

Aurash Khawarзад, PhD student

The Graduate Center at the City University of New York, Earth and Environmental Sciences dept

[akhawarзад@gradcenter.cuny.edu](mailto:akhawarзад@gradcenter.cuny.edu)

ORCID: 0009-0005-9428-8467

January 29, 2026

### **Abstract**

This paper presents a web-based research method for studying changes in vegetation in urban and suburban contexts between 2018 and 2024. The system uses the Normalized Difference Vegetation Index (NDVI) to analyze imagery for each period and classify land surface types. After classification, correlation and regression analysis are applied to explain connections between urbanization and vegetation change over time. Two case studies are included to demonstrate the method's validity: suburban Warrenton, Virginia and urban Portland, Oregon, which have contrasting physical characteristics and land use policies. By providing workflow documentation and using open source technology, this method democratizes land classification analysis for researchers in planning, conservation, and related fields. Potential improvements for this tool include: 1-higher resolution imagery; 2-conducting field research to verify results and build regional models; and 3-improve NDVI application for broader land classification results. The research method is available for public use at: <https://terrestrialresearch.com/machinelearning/landclass2>.

**Keywords:** open source GIS, remote sensing tools, vegetation growth analysis, land use/land cover change (LULCC) methodology, accessible research tools

### **Research application website**

<https://terrestrialresearch.com/machinelearning/landclass2>

### **Github repository**

<https://github.com/aurashak/ndvilandclass>

## **1. Introduction**

This paper presents a web-based method for analyzing vegetation change in urban and suburban contexts using publicly available satellite data and open source technology. Despite advances in remote sensing capabilities, accessible tools for land classification remain limited for researchers in policy, planning, design, and related fields who lack access to specialized software and hardware. The Normalized Difference Vegetation Index

(NDVI) (Tucker, 1979) is an established remote sensing metric that analyzes near-infrared and red wavelengths to identify surface types, with particular effectiveness for vegetation analysis (Goward, et al., 1991; Petorelli, et al., 2005).

This method addresses the accessibility gap by providing a documented workflow using the European Space Agency's Sentinel-2 satellite constellation (Drusch et al., 2012), a web-based mapping interface (Agafonkin, 2011), and Python geospatial libraries (Harris et al., 2020; Hunter, 2007; Virtanen et al., 2020) to classify land cover types and analyze vegetation change between 2018 and 2024. The system processes 512×512 pixel areas, classifying surfaces as water, bare/paved, sparse vegetation, moderate vegetation, or dense vegetation, then applies correlation and regression analysis to quantify relationships between urbanization and vegetation change. Case studies of Warrenton, Virginia and Portland, Oregon, are included to demonstrate the method's validity across contrasting landscapes.

### 1.1 Research Objectives

- Methodological framework: Provide detailed documentation for developing a land classification method using open data designed for urban and suburban contexts. The utilization of open data and open source technology makes this approach replicable and accessible.
- Validation: Conduct two example analyses demonstrating the method's application and reliability.
- Technical assessment: Document challenges and opportunities related to data quality, resolution, and long-term system maintenance.

## 2. Methods

### 2.1. Web Application Infrastructure

#### 2.1.1. Frontend Design

This system is divided between the frontend (HTML and JavaScript), where the viewer can select the location they want to apply the research method and view the maps, text, charts and other results; and the backend (Python), where scripts are executed that retrieve data from the web and apply the NDVI algorithm. Leaflet.js is used as open source mapping framework for displaying satellite data collected by Sentinel-2 (Agafonkin, 2011).

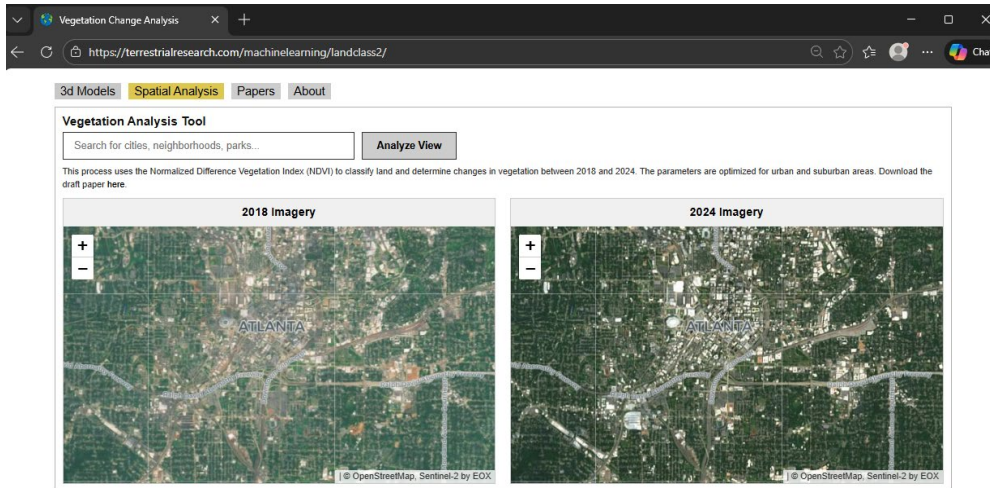


Figure 1: Land Classification Web Application.

### 2.2.2. Backend Computation

The Python script retrieves data from the Copernicus data hub via API, then accesses the Pillow, NumPy, Matplotlib, and SciPy libraries to conduct statistical analysis and produce data visualizations for the NDVI results (Harris et al., 2020; Hunter, 2007; Virtanen et al., 2020). These libraries provide the capabilities for processing satellite data, including massive tables and arrays containing billions of data points for geographic coordinates, color, height, and other data used in LULLC.

### 2.2.3. Code Development

Server infrastructure, web interface design, mapping framework implementation (Leaflet, QGIS), API connectivity (Copernicus), and statistical analysis methods were developed by the author. The open-source Large Language Model Qwen3-Coder assisted with code generation and debugging for Python and JavaScript components. All code was reviewed, edited, and implemented by the author.

## 2.2. Satellite Data Quality and Availability

This method uses imagery from the European Space Agency's Sentinel-2 satellite constellation, which provides publicly accessible multispectral data at 10 meter resolution (Drusch et al., 2012). The timeframe of 2018 to 2024 was selected because this represents the period of consistent, freely available 10 meter resolution data from the Copernicus program (Drusch, et al., 2012; European Space Agency, 2020). Earlier Sentinel-2 data (dating to 2015) exists but with inconsistent coverage (Verbesselt et al., 2010). While higher resolution commercial satellite imagery exists (up to 30 cm per pixel from providers like Maxar and Planet (EOPortal, 2025; Maxar Technologies, 2026), these data are not freely accessible via API, presenting technical barriers for creating publicly available research tools.

**2.3. Normalized Difference Vegetation Index (NDVI) and Land Classification** 108

**2.3.1. NDVI Formula and Application** 109

The near infrared (NIR) data that is analyzed by the NDVI is captured by multispectral cameras on the Sentinel-2 satellites. This web application allows the viewer to select a 512px by 512px area of the earth and to analyze each pixel in that section for near infrared and red band light using the formula (Tucker, 1979): 110-113

$$NDVI = \frac{(NIR - Red)}{(NIR + Red)}$$
 114-115

**2.3.2. Classification Thresholds** 116-117

The formula calculates a value between -1 to +1 for each pixel. Higher values within that range represent vegetation, while low and negative values typically represent water, bare soil, and paved surfaces (Pettoirelli et al., 2005). In this method, the Python script converts the NDVI value to a color range for visualization on the map. The values are converted into these categories and colors: 118-122

NDVI Range	Description	Color Code
< -0.1	Water	Blue
-0.1 to 0.2	Bare/Urban	Gray
0.2 to 0.35	Sparse Vegetation	Light Yellow
0.35 to 0.5	Moderate Vegetation	Light Green
≥ 0.5	Dense Vegetation	Dark Green

 123

**2.3.3. Surface Classification Scope** 124-125

This application focuses on land cover types typical in urban and suburban contexts. The classification excludes surfaces not commonly found in these environments (dense rain-forest, agricultural crop phases, deep water bodies, ice/snow cover) to optimize accuracy for the target surface types. This specialization makes the tool particularly suited for urban planning and design applications but limits applicability to other geographic contexts such as oceans, or dense tropical forests. Future enhancements using hyperspectral sensors with 100-200+ spectral bands (compared to Sentinel-2's 13 bands) could enable more detailed vegetation classification, including species identification and health assessment (NASA Jet Propulsion Laboratory, 2023). 126-134

**2.3.4. Scale of Imagery** 135-136

The NDVI algorithm performs optimally within specific elevation ranges based on sensor capabilities. This application uses Leaflet.js zoom controls to limit the camera view to elevations between approximately 1,800m and 2,200m (map scales of roughly 1:15,000 to 1:18,000). This constraint prevents mixture of surface types that reduce classification accuracy.

## 2.4. Statistical Analysis

As stated previously, the NDVI uses near infrared imagery data captured from satellites to create a value between -1 to 1 that it assigns to each pixel of the area being analyzed by the application, with the lower end of the spectrum representing unvegetated areas and the higher end representing vegetated areas (Tucker, 1979). The statistical analysis portion of this method compares the difference in value for each pixel between the imagery captured in 2018 and 2024 (Singh, 1989).

### 2.4.1. Change to Urban and NDVI Change

In this model, the independent variable is the "urban\_gain" value in the formula below, which is a 0 or 1 classification indicating whether a pixel changed to built environment. In Python the formula to determine this value is:

```
urban_gain = ((classes_2018 != 1) & (classes_2024 == 1)).astype(int)
```

The dependent variable is the difference in vegetation, measured as the continuous numerical change in NDVI values for that same pixel between the satellite images. The Python code used in this project to determine the change in NDVI value for each pixel is:

```
ndvi_change = ndvi_2024 - ndvi_2018
```

Using mathematical notation:

$$\Delta NDVI_i = NDVI_{2024,i} - NDVI_{2018,i}$$

Where:

$\Delta NDVI_i$  = change in NDVI for pixel i

$NDVI_{2024,i}$  = NDVI value for pixel i in 2024

$NDVI_{2018,i}$  = NDVI value for pixel i in 2018

By isolating these variables, the analysis can test the hypothesis that urban development and loss of vegetation are connected.

### 2.4.2. Pearson's r correlation coefficient

Once it is determined which pixels have transitioned from vegetated to paved/bare classification (urban\_gain) and the NDVI change for each pixel (ndvi\_change), a correlation analysis is done using the Pearson's r technique (Virtanen et al., 2020). This correlation analysis establishes if there is a link between urbanization and the decrease vegetation. Determining correlation is important because while simple land classification can show if vegetation is being lost, it does not mathematically prove the relationship to development. Pearson's r measures the relationship between urbanization and vegetation.

The formula for determining correlation (Pearson's r) is:

$$r = \frac{\Sigma[(x_i - \bar{x})(y_i - \bar{y})]}{\sqrt{\Sigma(x_i - \bar{x})^2 \cdot \Sigma(y_i - \bar{y})^2}}$$

Where:

$x_i$  = UrbanGain<sub>i</sub>

$y_i$  =  $\Delta$ NDVI<sub>i</sub>

$\bar{x}$  = mean of UrbanGain

$\bar{y}$  = mean of  $\Delta$ NDVI

This Python code determines the link between urban\_gain (x) and the ndvi\_change (y):

```
r_value, p_value = stats.pearsonr(urban_gain_valid, ndvi_change_valid)
```

The correlation coefficient (r) from that formula ranges from -1 to +1. In this study, a value near -1 indicates a strong inverse relationship, confirming that urban expansion is directly tied to vegetation loss. Conversely, a value of 0 would indicate no linear relationship between the two variables. A value of 1 would mean a positive correlation of both urban growth and vegetation growth. The p-value (p\_value), with a significance level of < 0.05, ensures the correlation is reliable (Virtanen et al., 2020).

### 2.4.3. Linear Regression

After establishing correlation through Pearson's r, a linear regression model is applied to quantify the level of NDVI change associated with urbanization. This regression measures exactly how much vegetation loss occurs when a pixel transitions to urban development (Virtanen et al., 2020). The Python implementation uses:

```
slope, intercept, r_val, p_val, std_err = stats.linregress(urban_gain_valid,
ndvi_change_valid)
```

The regression equation takes the form:

$$\text{NDVI Change} = \beta \times (\text{Urban Gain}) + \alpha$$

Where: 217  
 $\beta$  = slope (regression coefficient) 218  
 $\alpha$  = intercept 219

220  
The slope ( $\beta$ ) and intercept ( $\alpha$ ) are the two key parameters that define the linear relation- 221  
ship between urbanization and NDVI change. A negative slope shows that urbanization 222  
is causing loss of vegetation. The intercept represents the expected NDVI change for non- 223  
urban pixels (where urban\_gain = 0), establishing a baseline trend that accounts for natu- 224  
ral environmental variations unrelated to urbanization, such as changes in climate. 225

#### 2.4.4. R<sup>2</sup> Coefficient of Determination 226

227  
The coefficient of determination (R<sup>2</sup>) measures how well the regression model explains 228  
the observed data (Virtanen et al., 2020). It is calculated as the square of the correlation 229  
coefficient (r) obtained from the Pearson's r analysis in the previous step. R<sup>2</sup> indicates the 230  
proportion of NDVI variance explained by development. A higher R<sup>2</sup> value means that a 231  
greater percentage of observed vegetation change can be attributed specifically to urban 232  
expansion, while the remaining variance results from other factors such as climate or 233  
land management practices. The formula for this calculation is: 234

$$R^2 = r^2$$

235  
236  
237  
R<sup>2</sup> indicates the proportion of NDVI variance explained by development. A higher R<sup>2</sup> 238  
value means that a greater percentage of observed vegetation change can be attributed 239  
specifically to urban expansion. 240

241  
The p-value from the regression analysis, similar to the p-value from the correlation test, 242  
confirms the statistical significance of the relationship. 243

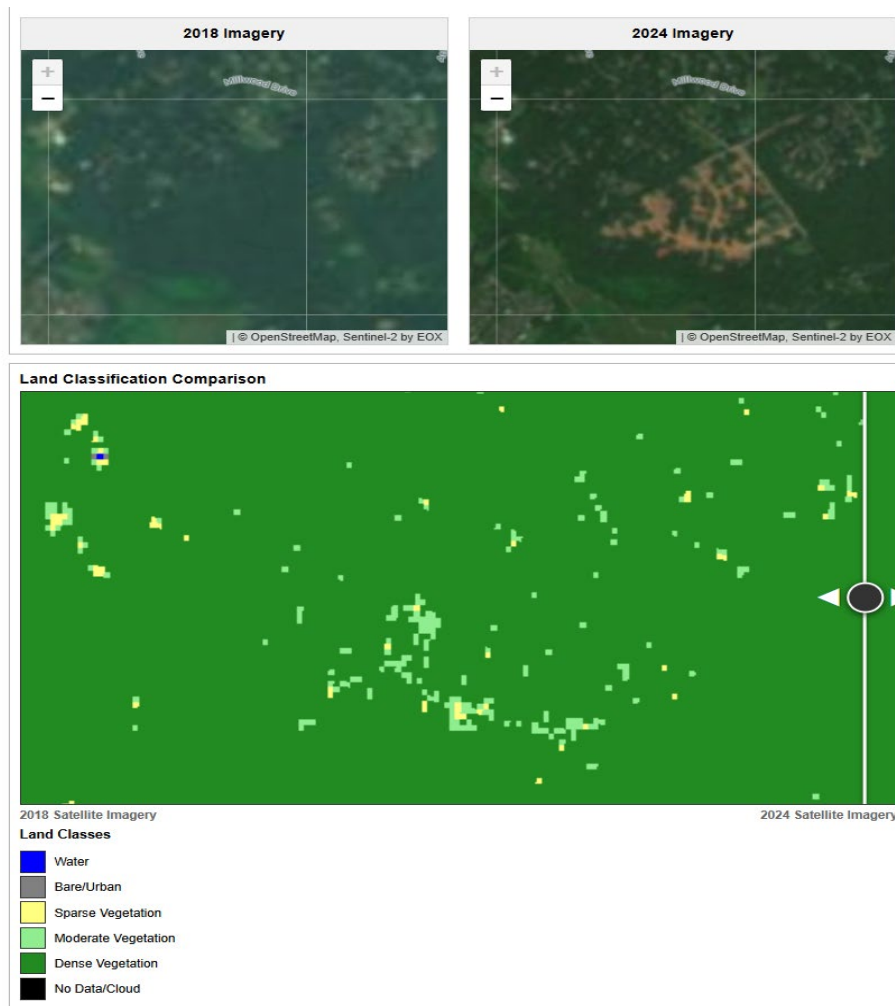
### 3. Results 244

245  
This paper includes analysis of two distinct regions to demonstrate performance across 246  
different contexts: a dense urban area growing through densification rather than sprawl, 247  
and a rural area experiencing rapid suburban style sprawl, with those areas being Port- 248  
land, Oregon; and Warrenton, Virginia, respectively. These locations were selected to 249  
represent contrasting approaches to urban growth and land use planning in the United 250  
States. These locations were also chosen for their vegetated conditions, which are easily 251  
recognizable by the Sentinel-2 MSI, as opposed to surfaces that may have snow or sand, 252  
which can require adjustment of the algorithm (Verbesselt et al., 2010). 253

#### 3.1. Study Area 1: Warrenton - Exurban Northern Virginia 254

255  
The municipality of Warrenton is located approximately 50 miles west of central Wash- 256  
ington D.C., within commuting distance of the metropolitan region's outer suburbs and 257

employment centers. The analyzed area covers approximately 0.64 square miles (1.65 square kilometers) in the 512 pixel by 512 pixel grid (for a total of 262,144 pixels analyzed). This specific section was selected because there are clear signs of land development occurring between the 2018 and 2024 capture periods of satellite imagery. It's clear that vegetation has been removed in a wide swath of territory. The suburban and exurban areas of Virginia were selected because they rank among the fastest growing suburbs in the United States for the study period - having added 90,000 residents between 2023-2024 alone (Wilder and Mackun, 2025).



267

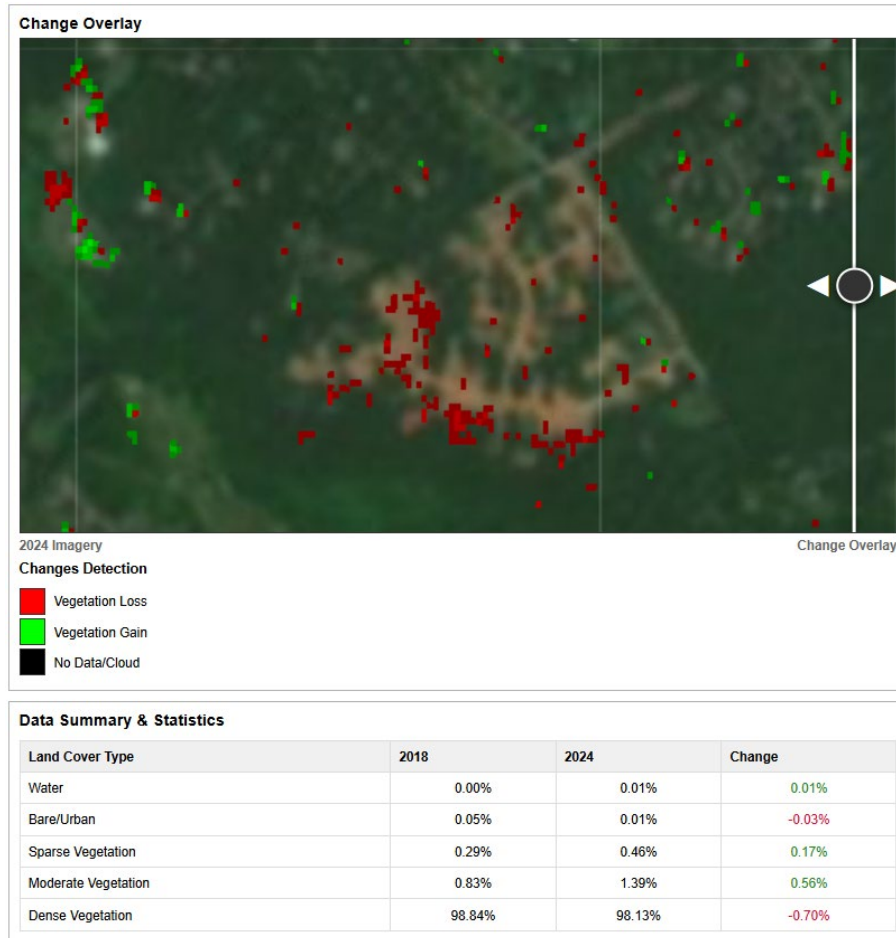


Figure 3: Warrenton, Virginia analysis.

Location analyzed: 38.719° to 38.730° N and longitudes 77.773° to 77.755° W.

The analysis does not directly classify new development but does show a notable decline in overall vegetation (NDVI). Mean NDVI dropped from 0.934 in 2018 to 0.843 in 2024, representing a decrease of -0.090 (approximately 9.7%). Even with the decline, the region remained forested, with dense vegetation comprising over 98% of land cover in both time periods. This reduction can be seen in the imagery where vegetation has been removed - although other areas may have grown more, thus compensating for the removal. The NDVI change range of -0.714 to +0.575 indicates substantial localized variation, with some areas experiencing severe vegetation loss while others showed improvement. It's also clear from the red pixel visualization that the algorithm does not identify all pixels that have lost vegetation but does show general trends.

The statistical relationship between development and vegetation change in the Warrenton analysis reveals a small negative correlation ( $r = -0.005$ ,  $R^2 = 0.0\%$ ). The regression model shows a negative slope ( $\beta = -1.081$ ), indicating that areas experiencing development averaged NDVI losses of -0.736 compared to gains of +0.344 in non-developed

268  
269  
270  
271  
272  
273  
274  
275  
276  
277  
278  
279  
280  
281  
282  
283  
284  
285  
286

areas. The changes in land classification show a minimal net change, over 90% of pixels remained in the same class, 4.5% gained vegetation, and 3.8% lost vegetation (Singh, 1989).

287  
288  
289  
290  
291  
292  
293  
294  
295  
296  
297  
298  
299

### 3.2. Study Area 2: Portland - Urban Core

The Portland metropolitan area was selected as a contrasting area due to its reputation for progressive land use planning policies, including an urban growth boundary (UGB) established in 1979, transit-oriented development (TOD) initiatives, and lauded sustainability programs (Metro, 2023; Abbott, 2001). The analyzed area covers approximately 1.4 square miles (3.6 square kilometers) or 262,144 pixels analyzed. This specific section was selected to examine vegetation dynamics in an urban core, where growth is occurring through densification and infill development rather than outward sprawl.



300

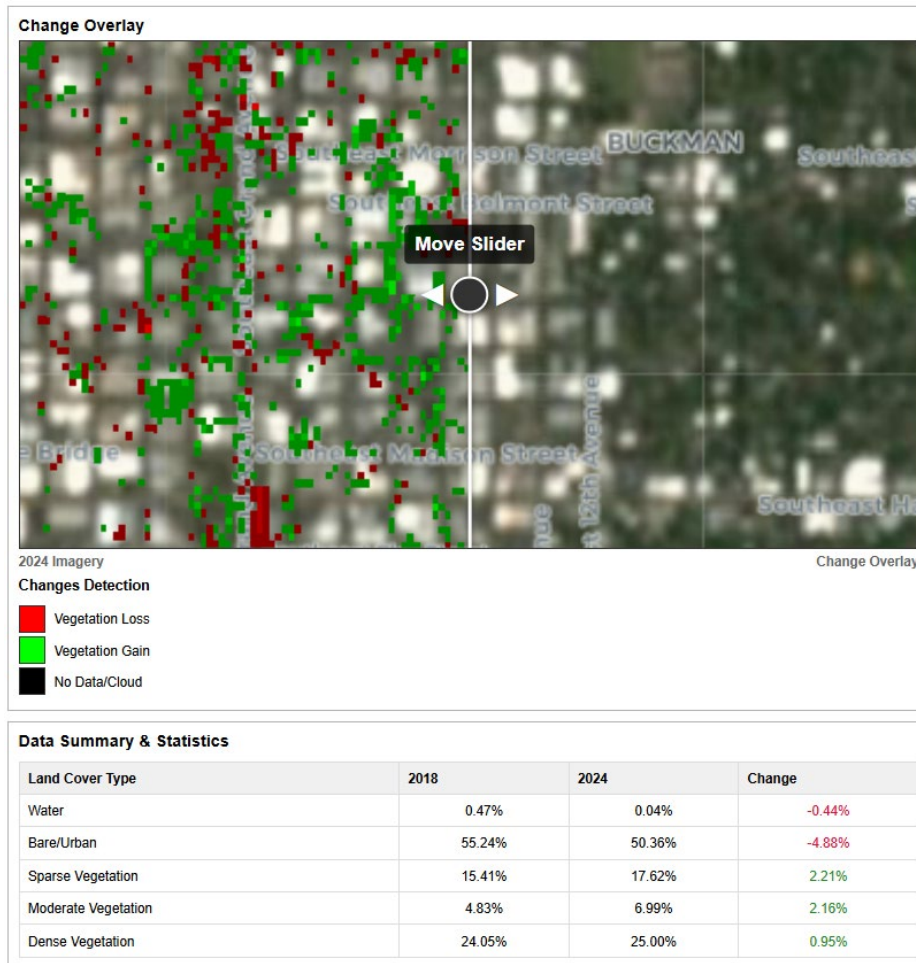


Figure 4: Portland, Oregon analysis

Location: latitudes 45.505° to 45.526° N and longitudes 122.667° to 122.631° W.

The statistical relationship between development and vegetation change in this part of Portland reveals a weak positive correlation ( $r = 0.095$ ,  $R^2 = 0.9\%$ ). The regression model shows a positive slope ( $\beta = 9.500$ ), indicating that areas experiencing development averaged NDVI gains of +9.533 compared to gains of +0.033 in non-developed areas. With 10,363 pixels (3.95%) classified as experiencing development, or urban gain, which are areas that transitioned to paved or bare surfaces, the urban expansion represents approximately 4% of the total study area. The changes in land classification shows a counter-intuitive change: bare/urban surfaces decreased from 55.2% to 50.4% (-4.8%), while vegetation coverage increased across all categories (sparse +2.2%, moderate +2.2%, dense +0.9%). When combined with knowledge that the population of the city grew during this period, this pattern suggests greening within the urban fabric rather than vegetation loss from development.

#### 4. Discussion

#### 4.1. Method Validation

To assess accuracy, results were compared against The National Land Cover Database (NLCD) from the U.S. Geological Survey (Homer et al., 2020). However, the most recent publicly available NLCD is from 2021, predating this study's 2024 analysis by three years, and uses 30-meter resolution compared to Sentinel-2's 10-meter resolution, limiting direct comparison.

The most definitive validation approach would involve field verification through direct observation at specific locations (ground-truthing). While beyond this study's scope, such field observations would verify the current approach and provide training data for developing region-specific classification models that account for local vegetation types, pavement characteristics, and weather patterns. The contrasting case studies presented here demonstrate the method's capability to detect distinct vegetation change patterns, supporting the tool's validity for comparative urban analysis.

#### 4.2. Applications

Specific applications of this method include monitoring tree planting programs, tracking urban tree canopy loss, identifying potential urban heat island zones, establishing baseline vegetation conditions for development projects, and documenting long-term climate impacts on urban ecosystems, among others.

The open source architecture and documented workflow enable researchers to replicate and adapt this method for different geographic regions. Code availability and reliance on freely accessible Sentinel-2 data through the Copernicus Open Access Hub eliminate cost barriers while maintaining scientific standards through the established NDVI methodology and statistical analysis techniques.

#### 4.3. Limitations and Future Enhancements

Current limitations stem primarily from Sentinel-2's 10-meter resolution, which may not detect small vegetated features such as street trees, or small parks and home gardens. Future enhancements could include: 1) integration of ground reference data to develop region-specific classification models accounting for local vegetation types and surface characteristics; 2) incorporation of higher-resolution imagery as it becomes publicly available; and 3) expansion to hyperspectral sensors from upcoming missions such as ESA's CHIME (Copernicus Hyperspectral Imaging Mission for the Environment) and NASA's Surface Biology and Geology mission (NASA Jet Propulsion Laboratory, 2023), which will enable species-level vegetation identification and detailed ecosystem mapping.

The methodology presented here establishes a foundation that can evolve as sensor technology advances and computing capabilities expand, while maintaining its core principle of accessibility through open data and open source tools.

## 5. Conclusions 362

This paper demonstrates an accessible methodology for analyzing land use and land cover change at the urban and suburban scale using Sentinel-2 satellite imagery and NDVI classification programs. The tool democratizes remote sensing analysis for researchers across multiple disciplines by not requiring specialized software or large budgets. Through case studies of Warrenton, Virginia and Portland, Oregon, the method successfully detected contrasting patterns of vegetation change associated with different urban development approaches - suburban sprawl versus urban densification. 363  
364  
365  
366  
367  
368  
369

While the current version has limitations in spatial resolution and temporal coverage, the methodology provides a foundation that can be enhanced as newer datasets from more advanced sensors become publicly available. The statistical framework incorporating correlation and regression analysis adds rigor beyond simple visual study, allowing researchers to determine relationships between development and vegetation change. Future improvements through ground-truthing and enhanced satellite data could strengthen the applicability of this approach for urban planning, conservation, and environmental monitoring applications. 370  
371  
372  
373  
374  
375  
376  
377  
378

### Code and Data Availability 379

The web application is publicly accessible at: <https://terrestrialresearch.com/machinelearning/landclass2> 380  
381  
382

Source code is available at: <https://github.com/aurashak/ndvilandclass> 383

Data used in this study is freely available through the Copernicus Open Access Hub: <https://scihub.copernicus.eu/> 384  
385  
386

### Data and Software 387

Satellite imagery data were provided by the ESA via the Copernicus Open Access Hub. The author acknowledges the open source software communities that developed and maintain the Python libraries (NumPy, SciPy, Matplotlib, Pillow), JavaScript frameworks (Leaflet.js), and geospatial tools (QGIS) used in this research. Free and open source Large Language Models were used to assist with web development as described in Section 2.2.3. 388  
389  
390  
391  
392  
393

### Abbreviations 394 395

API	Application Programming Interface	396
CHIME	Copernicus Hyperspectral Imaging Mission for the Environment	397
ESA	European Space Agency	398
GIS	Geographic Information System	399
LULCC	Land Use/Land Cover Change	400

MSI	Multi-Spectral Instrument	401
NASA	National Aeronautics and Space Administration	402
NDVI	Normalized Difference Vegetation Index	403
NIR	Near Infrared	404
NLCD	National Land Cover Database	405
R <sup>2</sup>	Coefficient of Determination	406
RGB	Red, Green, Blue (visible light spectrum)	407
SBG	Surface Biology and Geology (mission)	408
USGS	United States Geological Survey	409
VHR	Very High Resolution	410

## Bibliography

1. Agafonkin, V. (2011). Leaflet: An open-source JavaScript library for mobile-friendly interactive maps. Available at: <https://leafletjs.com> 413-414
2. Abbott, C. (2001) *Greater Portland: Urban Life and Landscape in the Pacific Northwest*. Philadelphia: University of Pennsylvania Press. 415-416
3. Drusch, M., Del Bello, U., Carlier, S., Colin, O., Fernandez, V., Gascon, F., ... & Bargellini, P. (2012). Sentinel-2: ESA's optical high-resolution mission for GMES operational services. *Remote Sensing of Environment*, 120, 25-36. <https://www.sciencedirect.com/science/article/abs/pii/S0034425712000636> 417-419
4. EOportal (2025). *WorldView Legion Specifications*. <https://www.eoportal.org/satellite-missions/worldview-legion> 421-422
5. European Space Agency (2025). *S2 Mission - SentiWiki*. <https://sentiwiki.copernicus.eu/web/s2-mission> 423-424
6. ESA (European Space Agency). (2024). Sentinel-2C joins the Copernicus family in orbit. [https://www.esa.int/Applications/Observing\\_the\\_Earth/Copernicus/Sentinel-2/Sentinel-2C\\_joins\\_the\\_Copernicus\\_family\\_in\\_orbit](https://www.esa.int/Applications/Observing_the_Earth/Copernicus/Sentinel-2/Sentinel-2C_joins_the_Copernicus_family_in_orbit) 425-427
7. Google Earth (2025) Google Earth. <https://earth.google.com> 428
8. Goward, S.N., Markham, B., Dye, D.G., Dulaney, W., & Yang, J. (1991). Normalized difference vegetation index measurements from the Advanced Very High Resolution Radiometer. *Remote Sensing of Environment*, 35(2-3), 257-277. <https://www.sciencedirect.com/science/article/abs/pii/003442579190017Z> 429-432
9. Harris, C.R., Millman, K.J., van der Walt, S.J., Gommers, R., Virtanen, P., Cournapeau, D., ... & Oliphant, T.E. (2020). Array programming with NumPy. *Nature*, 585(7825), 357-362. <https://www.nature.com/articles/s41586-020-2649-2> 433-435
10. Homer, C., Dewitz, J., Jin, S., et al. (2020). Conterminous United States land cover change patterns 2001–2016 from the 2016 National Land Cover Database. *ISPRS Journal of Photogrammetry and Remote Sensing*, 162, 184-199. <https://www.sciencedirect.com/science/article/pii/S0924271620300587> 436-439
11. Hunter, J.D. (2007). Matplotlib: A 2D graphics environment. *Computing in Science & Engineering*, 9(3), 90-95. <https://ieeexplore.ieee.org/document/4160265> 440-441

12. Lunetta, R.S., Knight, J.F., Ediriwickrema, J., Lyon, J.G., & Worthy, L.D. (2006). Land-cover change detection using multi-temporal MODIS NDVI data. *Remote Sensing of Environment*, 105(2), 142-154. <https://www.sciencedirect.com/science/article/abs/pii/S0034425706002549>
13. Metro. (2023). Urban Growth Boundary. Portland Metro Regional Government. <https://www.oregonmetro.gov/what-metro-does/land-use-and-development/2040-growth-concept/urban-growth-boundary>
14. NASA Jet Propulsion Laboratory (2023) *Surface Biology and Geology (SBG)*. <https://sbg.jpl.nasa.gov/>
15. Pettorelli, N., Vik, J.O., Mysterud, A., Gaillard, J.M., Tucker, C.J., & Stenseth, N.C. (2005). Using the satellite-derived NDVI to assess ecological responses to environmental change. *Trends in Ecology & Evolution*, 20(9), 503-510.
16. Qwen Team. (2023). *Qwen Coder*. Available at: <https://github.com/QwenLM/Qwen-Coder> [accessed on: November 2023]
17. Romaniuk, Paweł & Saeed, Khalid & Boucetta, Rahma. (2023). *Exploring Object Size Estimation Through Low-Cost Drone Technology*. [https://www.researchgate.net/publication/371703546\\_Exploring\\_Object\\_Size\\_Estimation\\_Through\\_Low-Cost\\_Drone\\_Technology](https://www.researchgate.net/publication/371703546_Exploring_Object_Size_Estimation_Through_Low-Cost_Drone_Technology)
18. Singh, A. (1989). Digital change detection techniques using remotely-sensed data. *International Journal of Remote Sensing*, 10(6), 989-1003. <https://www.tandfonline.com/doi/abs/10.1080/01431168908903939>
19. Tucker, C.J. (1979). Red and photographic infrared linear combinations for monitoring vegetation. *Remote Sensing of Environment*, 8(2), 127-150. <https://www.sciencedirect.com/science/article/abs/pii/0034425779900130>
20. Verbesselt, J., Hyndman, R., Newnham, G., & Culvenor, D. (2010). Detecting trend and seasonal changes in satellite image time series. *Remote Sensing of Environment*, 114(1), 106-115. <https://www.sciencedirect.com/science/article/abs/pii/S003442570900265X>
21. VanderPlas, J. (2016). *Python Data Science Handbook: Essential Tools for Working with Data*. O'Reilly Media. <https://jakevdp.github.io/PythonDataScienceHandbook/>
22. Virtanen, P., Gommers, R., Oliphant, T.E., Haberland, M., Reddy, T., Cournapeau, D., ... & SciPy 1.0 Contributors. (2020). SciPy 1.0: fundamental algorithms for scientific computing in Python. *Nature Methods*, 17(3), 261-272. <https://www.nature.com/articles/s41592-019-0686-2>
23. Wilder, K. and Mackun, P. (2025). U.S. Metro Areas Experienced Population Growth Between 2023 and 2024. <https://www.census.gov/library/stories/2025/04/metro-area-trends.html>